ELSEVIER

Neurobiology of Aging 31 (2010) 1304–1311

NEUROBIOLOGY OF AGING

www.elsevier.com/locate/neuaging

Subregions of the inferior parietal lobule are affected in the progression to Alzheimer's disease

Sarah J. Greene[a], Ronald J. Killiany[a,b,c,*], The Alzheimer's Disease Neuroimaging Initiative[†]

[a] *Department of Anatomy and Neurobiology, Boston University School of Medicine, Boston, MA 02118, USA*
[b] *Center for Biomedical Imaging, Boston University School of Medicine, Boston, MA, 02118, USA*
[c] *Department of Environmental Health, Boston University School of Public Health, Boston, MA, 02118, USA*

Received 12 February, 2010; received in revised form 23 April 2010; accepted 23 April 2010

Abstract

Changes in several regions within the brain have been associated with progression from healthy aging to Alzheimer's disease (AD), including the hippocampus, entorhinal cortex, and the inferior parietal lobule (IPL). In this study, the IPL was divided into three subregions: the gyrus, the banks of the sulcus, and the fundus to determine if these regions are independent of medial temporal regions in the progression of AD. Participants of the Alzheimer's disease Neuroimaging Initiative (Alzheimer's disease Neuroimaging initiative (ADNI); n = 54) underwent a structural magnetic resonance imaging (MRI) scan and neuropsychological examination, and were categorized as normal controls, mild cognitively impaired (MCI), or AD. FreeSurfer was initially used to identify the boundaries of the IPL. Each subregion was then manually traced based on FreeSurfer curvature intensities. Multivariate analyses of variance were used to compare groups. Results suggest that changes in thickness of the banks of the inferior parietal lobule are occurring early in the progression from normal to MCI, followed by changes in the gyrus and fundus, and these measures are related to neuropsychological performance.

Keywords: Alzheimer's disease; Mild cognitively impaired; Magnetic resonance imaging; Inferior parietal lobule

Alzheimer's disease (AD) is the most common form of dementia, and is the fifth leading cause of death in individuals over the age of 65. There are no definitive means for detecting who will develop AD. Magnetic resonance imaging (MRI) has provided a useful *in vivo* method for assessing changes that occur in the brain during the progression from healthy aging to AD, and offers potential means for identifying individuals in the presymptomatic stages, where treatment may delay or prevent the onset of this disease. MRI also offers the ability to track AD over time. As MRI postprocessing techniques have been improved, the investigation of markers for development and progression to Alzheimer's disease has advanced. Several regions of interest have been intensely studied in subjects with both mild cognitively impaired (MCI) and AD, such as the hippocampus and entorhinal cortex. More recently, regions beyond the medial temporal lobe such as the inferior parietal lobule (IPL) have begun to show promise as markers of AD.

The inferior parietal lobule is defined in this study as the lateral region of the parietal lobe extending between the supramarginal gyrus rostrally, the lateral occipital cortex caudally, the superior parietal gyrus medially, and the middle temporal gyrus laterally (Desikan et al., 2006). Functionally, the IPL is involved with sensory and motor association. Both amyloid plaques and neurofibrillary tangles have been found at the time of autopsy in the IPL in MCI and AD subjects (Braak and Braak, 1991; Markesbery et al.,

* Corresponding author at: Department of Anatomy and Neurobiology, Boston University School of Medicine, 700 Albany Street, W701, Boston, MA 02118, USA. Tel.: (617) 638-8082; fax: (617) 638-4922.
E-mail address: Killiany@bu.edu (R.J. Killiany).

[†] Data used in the preparation of this article were obtained from the Alzheimer's disease Neuroimaging Initiative (ADNI) database (www.loni.ucla.edu/ADNI). As such, the investigators within the ADNI contributed to the design and implementation of ADNI and/or provided data but did not participate in analysis or writing of this report. A complete listing of ADNI investigators is available at www.loni.ucla.edu/ADNI\Collaboration\ADNI_Authorship_list.pdf.

0197-4580/$ – see front matter © 2010 Elsevier Inc. All rights reserved.
doi:10.1016/j.neurobiolaging.2010.04.026

2006; Nelson et al., 2009). Studies in nonhuman primates have demonstrated connections between the IPL and both the entorhinal cortex (Ding et al., 2000; Van Hoesen and Pandya, 1975), and the hippocampus (Clower et al., 2001), suggesting that the IPL is a part of the memory circuitry. As such, pathology in this region may be contributing to the memory impairment that is a hallmark of AD.

MCI is thought to represent a preclinical stage of AD (Bennett et al., 2005; Morris et al., 2001; Petersen et al., 2006; Whitwell et al., 2007). Studies have found atrophy of parietal regions in the presymptomatic stages of AD (Desikan et al., 2009; Fan et al., 2008; Fox et al., 2001; Scahill et al., 2002; Whitwell et al., 2008), and increased rates of atrophy in this region have been associated with conversion from MCI to AD (Desikan et al., 2008). Metabolic function in the IPL combined with genetic risk (carrying at least one copy of the APOE-4 allele) has been found to predict subsequent cognitive decline in normal subjects (Small et al., 2000). In addition, differences in blood flow to the IPL have been found in AD subjects both during rest (Scarmeas et al., 2004) and when performing memory tasks (Remy et al., 2005).

Because the IPL is a rather large structure, the purpose of this study was to determine if subregions within the IPL are differentially affected in the progression from normal to AD. In this study, the IPL was subdivided into the gyrus (G-IPL), the banks (B-IPL), and the fundus (F-IPL) based MRI measurements in normal (NC), MCI, and AD participants of the Alzheimer's disease Neuroimaging Initiative.

1. Methods

1.1. Study population

Data used in the preparation of this article were obtained from the Alzheimer's disease Neuroimaging Initiative (ADNI) database (www.loni.ucla.edu/ADNI). The ADNI was launched in 2003 by the National Institute on Aging (NIA), the National Institute of Biomedical Imaging and Bioengineering (NIBIB), the Food and Drug Administration (FDA), private pharmaceutical companies, and nonprofit organizations, as a US$60mn, 5-year public-private partnership. The primary goal of ADNI has been to test whether serial MRI, positron emission tomography (PET), other biological markers, and clinical and neuropsychological assessment can be combined to measure the progression of MCI and early AD. Determination of sensitive and specific markers of very early AD progression is intended to aid researchers and clinicians to develop new treatments and monitor their effectiveness, as well as lessen the time and cost of clinical trials.

The Principle Investigator of this initiative is Michael W. Weiner MD, VA Medical Center and University of California, San Francisco. ADNI is the result of the efforts of many coinvestigators from a broad range of academic institutions and private corporations, and subjects have been recruited from over 50 sites across the USA and Canada. The initial goal of ADNI was to recruit 800 adults, ages 55 to 90, to participate in the research—approximately 200 cognitively normal older individuals to be followed for 3 years, 400 people with MCI to be followed for 3 years, and 200 people with early AD to be followed for 2 years.

The inclusion criteria for each group are as follows: NC: Mini Mental Status examination (MMSE; Folstein et al., 1975) scores between 24 and 30, a Clinical Dementia Rating scale (clinical dementia rating (CDR)) (Morris, 1993) of 0, nondepressed, non-MCI, and nondemented; MCI (amnestic and multiple domain with memory impairment): subjective and objective memory complaint, MMSE scores between 24 and 30, objective memory loss measured by education adjusted scores on Wechsler Memory Scale Logical Memory II, a CDR of 0.5, absence of significant levels of impairment in other cognitive domains, essentially preserved activities of daily living, absence of dementia; AD (mild): MMSE scores between 20 and 26, CDR of 0.5 or 1.0, and meets NINCDS/ADRDA criteria (McKhann et al., 1984) for probable AD.

Participants underwent a neuropsychological battery at screening and MRI scanning at baseline, which are the data being evaluated in this study. Fifty-four participants (18 NC [55% female, average age 78.3], 18 MCI [50% female, average age 76.9], 18 AD [50% female, average age 76.6]) were pseudorandomly selected (randomly selected from within each group by gender) from the larger pool of approximately 800 baseline scans in the ADNI to be included in the current study. The operator was blind to gender and group membership. Demographics, including age, education, and MMSE were available for all 54 participants included in this study (Table 1).

1.2. Magnetic resonance imaging acquisition and postprocessing techniques

The imaging methods used by the ADNI have been described in detail previously (Jack et al., 2008). Scans were acquired from three manufacturers (General Electric Healthcare, Siemens Medical Solutions and Philips Medical Systems) using calibration techniques to maintain consistent protocols across scanners and sites. Raw dicom data of T1-weighted MP-RAGE scans acquired from 1.5 Tesla scanners at baseline visits from all 54 participants were

Table 1
Demographics

	Normal	MCI All	MCI Stable	MCI Converters	AD
Gender	55% F	50% F	39% F	80% F	50% F
Age	78.3	76.9	79	71.3	76.7
Education	16.3	15.9	15.2	17.8	15.1
MMSE	29.4	26.7	26.8	26.4	23.1

Demographics on 54 participants of the ADNI based on group membership. MCI subjects are subdivided into stable and converter groups.

obtained via the ADNI database (www.loni.ucla.edu/ADNI/). Images were processed through FreeSurfer version 4.0.3a software program freely available at surfer.nmr.mgh.harvard.edu/, to obtain measurements of the IPL. The details of this postprocessing program have been described elsewhere (Dale and Sereno, 1993; Dale et al., 1999; Fischl and Dale, 2000; Fischl et al., 1999a; Fischl et al., 1999b; Fischl et al., 2001; Fischl et al., 2002; Fischl et al., 2004a; Fischl et al., 2004b; Han et al., 2006; Jovicich et al., 2006; Segonne et al., 2004). Briefly, images were motion-corrected, intensity normalized using nonparametric, nonuniform (N3) correction (Sled et al., 1998), and stripped of nonbrain tissue (Segonne et al., 2004). Images underwent a subcortical segmentation (Fischl et al., 2002; Fischl et al., 2004a), identification of the gray/white matter boundary, automated topography correction (Fischl et al., 2001; Segonne et al., 2007), and surface deformation (Dale and Sereno, 1993; Dale et al., 1999; Fischl and Dale, 2000). Surface representation was reviewed by an anatomically trained operator (SJG), and edits to ensure accurate surfaces were completed where necessary.

Once reviewed, further processing was completed, including surface inflation (Fischl et al., 1999a), registration to a neuroanatomical atlas based on cortical folding patterns (Desikan et al., 2006; Fischl et al., 1999a; Fischl et al., 2004b), and maps of curvature and sulcal depth. The boundaries of each region of interest within the neuroanatomical atlas were visually inspected by the same neuroanatomically trained operator (SJG), and edits to these boundaries were completed where needed. This produced measurements of several neocortical and non-neocortical regions of interest, including the inferior parietal lobule, entorhinal cortex, hippocampus, and intracranial volume (ICV).

The boundaries of the IPL in this neuroanatomical atlas have been previously described (Desikan et al., 2006). This region of interest was manually subdivided into three regions by simultaneously viewing the neuroanatomical parcellation atlas and binary gray curvature maps on the inflated brain. The operator first manually traced the banks followed by the fundus of the right and left IPL by setting the curvature threshold to 0.0 and 0.55, respectively. The remainder of the IPL was then relabeled the gyrus of the IPL (Figure 1). Intrarater reliability was established by retracing these regions in a subset of participants (n = 5), which demonstrated a correlation of 0.99 between tracings. This provided measurements of total surface area (TSA), average cortical thickness (ACT), and total gray matter volume (GMV) for each of the three subregions of the IPL: G-IPL, B-IPL, and F-IPL.

The GMV, TSA, and ACT of each IPL subregion, the entorhinal cortex, hippocampus, and neuropsychological (NP) performance were compared between groups using separate MANOVAs followed by Tukey pairwise comparisons when appropriate. Pearson correlations were used to determine the magnitude of the linear relationships between morphometric measures and neuropsychological performance. A principle components analysis was completed to determine which neuropsychological measures would be included in these correlations. Discriminant Function Analyses were used to determine the best predictors of group membership (NC, MCI, and AD) and converters versus nonconverters in the MCI group.

1.3. Neuropsychological battery

The MMSE and Wechsler Memory Scale – Revised Logical Memory Immediate and Delayed (Wechsler, 1987) were administered at the screening visit. At the baseline visit, a battery of neuropsychological tests was given to all participants. This consisted of Alzheimer's disease Assessment Scale Cognitive examination (Rosen et al., 1984), Clock Drawing Test, Auditory Verbal Learning test (AVLT) (Rey, 1964), Digit Span Forward and Backward, Category Fluency, Trail making A and B (Reitan, 1958), Wechsler Adult Intelligence Scale-Revised (WAIS-R) Symbol Digit Substitution, Boston Naming Test (Kaplan et al., 1983), AVLT 30-minute delay, and the American National Adult Reading Test.

2. Results

Kruskal–Wallis one-way analyses of variance were used to demonstrate that groups did not significantly differ in gender, age, or education. The MRI variables were compared using multivariate analyses of variance. It was found that except for the GMV of the fundus of the IPL in the right hemisphere, all GMV and ACT measures were significantly

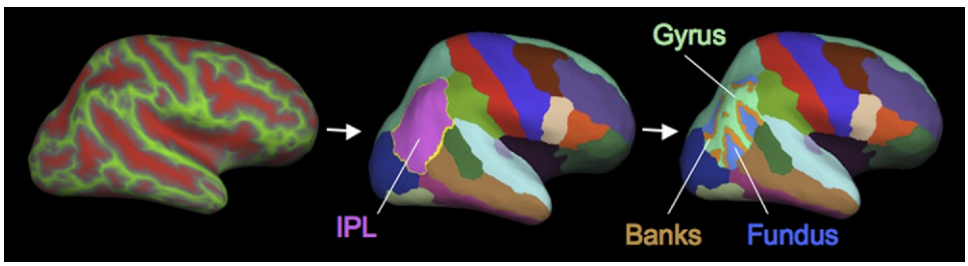

Fig. 1. Methods for manual tracing of each subregion of the inferior parietal lobule. First the sulcul-gyral pattern was loaded with the FreeSurfer parcellation atlas on the inflated brain, each subregion was then manually traced, and these subregions were then displayed with the parcellation atlas.

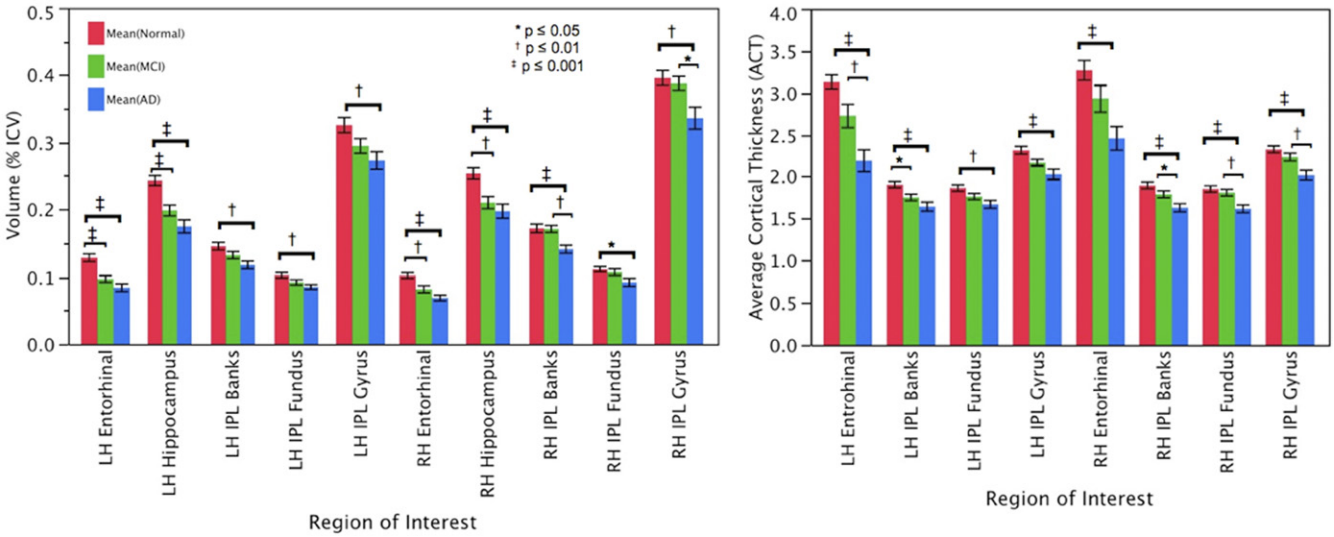

Fig. 2. (a) Differences between NC, MCI, and AD in volume of the left and right subregions of the IPL, hippocampus, and entrohinal cortex. Volumes are expressed as percent intracranial volume (% ICV). (b) Differences between NC, MCI, and AD in thickness of the left and right subregions of the IPL and entorhinal cortex.

different between groups in both the right and left hemisphere ($p < 0.01$). No TSA measures demonstrated a significant difference between groups.

Results of the Tukey pairwise comparisons (Figure 2a) revealed more insight into these differences. When comparing volume in the right hemisphere, G-IPL was significantly different between NC and AD and MCI and AD; B-IPL was significantly different between NC and AD and MCI and AD; and F-IPL was significantly different between NC and AD. In the left hemisphere, GMV was significantly different for G-IPL between NC and AD; B-IPL was significantly different between NC and AD; and F-IPL was significantly different between NC and AD.

When comparing thickness in regions of the right hemisphere (Figure 2b), G-IPL was significantly different between NC and AD and MCI and AD; B-IPL was significantly different between NC and AD and MCI and AD; and F-IPL was significantly different between NC and AD and MCI and AD. When comparing ACT in regions in the left hemisphere, G-IPL was significantly different between NC and AD; B-IPL was significantly different between NC and AD and NC and MCI; and F-IPL was significantly different between NC and AD. Because the main effect of group was not significant for the TSA measures, no follow up comparisons were made.

NP scores and p values demonstrating significant differences in NP performance are presented in Table 2. Traditionally NP tests have been portrayed as representing separate cognitive domains. Yet within each of the domain, subdomains exist (i.e. cognitive flexibility v. set maintenance as subcomponents of executive function), NP tests have some crossover between domains and it is never fully clear how each subdomain is affected by disease. To overcome these concerns, and to ensure that we understood how the various tests were inter-related in this dataset, a principle components analysis was used as a screening/data reduction tool to determine which of the NP tests to include in correlational analyses with the morphometric measurements. This broke the data down into three factors. The first factor consisted of Auditory Verbal Learning Immediate and Delay, the Boston Naming Test, and Categories; the second factor consisted of Trails A and Trails B, Digit Symbol, and Clock Command; and the third factor consisted of Trails B, Clock Command, Digit Span Forward, and Digit Span Backward. Scores from tests within each factor were selected for correlations in contrast to composite scores so that only known neuropsychological tests were evaluated. These included Clock Command, Auditory Verbal Learning Immediate and Delay, Digit Span Backward, Trails B, and Digit Symbol. Results of Pearson correlations were as follows ($p < 0.01$): LH GMV of IPL gyrus: Auditory Verbal Learning Delay; LH ACT of IPL gyrus: Auditory Verbal Learning Delay; LH ACT of IPL Banks: Auditory Verbal Learning Delay; LH GMV of IPL fundus: Auditory Verbal Learning Immediate, Trails B, and Digit Symbol; RH ACT of IPL gyrus: Auditory Verbal Learning Delay and Digit Symbol; RH ACT of IPL Banks: Auditory Verbal Learning Delay and Digit Symbol; RH ACT of IPL fundus: Auditory Verbal Learning Delay.

All regions of the IPL (RH and LH) and NP scores were entered into a discriminant function analysis to determine the best predictors of group membership, which revealed these were a combination of Auditory Verbal Learning Delay, Digit Symbol, and GMV of the banks of the right IPL, which were able to predict NC, MCI, and AD with

Table 2
Neuropsychological performance: differences between groups

Test	Group Mean			*p*-values		
	Normal	MCI	AD	Normal v. MCI	MCI v. AD	Normal v. AD
Clock Command (out of 5)	4.67	4.33	3.33	0.483	0.003	0.000
Clock Copy (out of 5)	4.78	4.72	4.44	0.964	0.405	0.276
AV Immediate 1 (out of 15)	4.94	4.28	3.11	0.424	0.080	0.003
AV Immediate 2	7.39	5.17	4.22	0.001	0.246	0.000
AV Immediate 3	9.50	6.44	4.50	0.001	0.040	0.000
AV Immediate 4	10.61	7.06	4.89	0.000	0.018	0.000
AV Immediate 5	11.39	7.06	5.06	0.000	0.056	0.000
AV Interference	4.72	4.00	3.00	0.226	0.063	0.001
AV Immediate 6	8.61	2.83	1.67	0.000	0.401	0.003
AV 30 min delay	12.72	8.61	6.17	0.004	0.123	0.000
Digit Span Forward	9.11	8.06	8.06	0.248	1.000	0.248
Digit Span Backward	7.39	6.28	5.33	0.224	0.339	0.009
Categories-Animals	19.56	16.50	12.56	0.193	0.069	0.001
Categories-Vegetables	15.44	10.61	8.22	0.001	0.157	0.000
Trails A (time to complete)	32.06	39.61	52.50	0.302	0.036	0.001
Trails B* (time to complete)	100.89	111.44	198.59	0.0904	0.003	0.001
Digit Symbol*	48.11	38.67	29.12	0.019	0.020	0.000
Boston naming Test*	27.94	24.50	20.82	0.094	0.074	0.000

The neuropsychological (NP) performance on each subtest of the NP battery was compared using MANOVA with Tukey follow-up comparisons. The group mean and *p*-values are listed for comparisons between normal and MCI, MCI and AD, and normal and AD participants. One AD subject is missing from comparisons.

83.3%, 61.1% and 77.8% accuracy, respectively. The diagnoses of MCI subjects at future visits were evaluated, and five of the 18 MCI subjects in this study converted to AD between the 12–18 month visit. The same variables were entered into a second discriminant function analysis to determine the best predictors for future conversion from MCI to AD, which were the Boston Naming Test, Digit Span Backwards, and GMV of the fundus of the right IPL, which were able to predict stable MCI and converters with 92.3% and 100% accuracy, respectively.

When combined with measures of the hippocampus and entorhinal cortex, the measures that were most able to discriminate between NC, MCI, and AD were a combination of the GMV of the left entorhinal cortex, GMV of the right banks of the IPL, and ACT of the left entorhinal cortex, which were able to determine group membership with 66.7%, 50%, and 83.3%, respectively. When these measures were combined with total scores on the NP examination, group membership was best predicted for NC, MCI, and AD with Auditory Verbal Learning Delay, left hippocampus, GMV of the right banks of the IPL, and Digit Symbol, which were able to predict group membership with 88.9%, 72.2%, and 70.6% accuracy, respectively.

When assessing measures of the entorhinal cortex, hippocampus, and IPL subregions in MCI subjects, the measure that was able to predict stable versus converters was the TSA of the left entorhinal cortex, which was able to predict group membership with 84.6% and 80% accuracy, respectively.

3. Discussion

Little is known of how subregions of the IPL may be differentially affected in the progression to AD. In this study, three subregions of the IPL were compared among normal, MCI, and AD subjects. The first objective was to determine if these subregions of the IPL are differentially affected in the progression from normal to AD. Results suggest that not only are these regions differentially affected in the group of participants investigated, but also they are differentially affected in the right and the left hemisphere. Results also suggest that measures of these subregions of the IPL contribute information related to MCI and AD that is independent of entorhinal and hippocampal measures.

When comparing normal to MCI subjects, only one subregion of the IPL was found to differ between these groups, suggesting that the banks of the left IPL may be affected before the involvement of the gyrus and the fundus. In addition, while both the GMV and ACT demonstrated significant differences between groups, there were no significant differences between groups when assessing TSA. Because GMV is derived from the ACT and TSA measures this suggests that the differences in the GMV are driven by thickness changes rather that changes in surface area.

Few studies have addressed functional differences in the gyrus, banks, and fundus of the inferior parietal lobule. One study evaluated the contribution of regions of the parietal lobe in number processing (Chochon et al., 1999), and found that the banks of the intraparietal sulcus and deep portion of the postcentral sulcus are activated in number processing tasks, suggesting that these subregions may have unique functional roles in cognition. The present study identified differing relationships between the gyrus, banks, and fundus of the IPL in the right and left hemisphere and cognitive performance. It was found that while several subregions in both hemispheres were associated with performance on memory tasks, only a select few were associated

with tasks involving numbers, including Digit Symbol (ACT of right gyrus and banks; GMV of left fundus) and Trails B (GMV of left fundus). This further suggests that these subregions may be functionally different, and therefore differentially affected in the progression to AD.

One further possibility is that these regions may be differentially affected due to perfusion differences in the gyrus, banks, and fundus of the IPL. Hypoperfusion of the inferior parietal region has been demonstrated in AD subjects when compared with those with MCI (Devanand et al., 2006; Grossman et al., 1997; Tranfaglia et al., 2009), and this may predict future progression from MCI to AD (Schroeter et al., 2009). It is possible that if this hypoperfusion is occurring differentially within the gyrus, banks, and sulcus of the IPL, this may contribute to differential effects in the progression from MCI to AD, contributing to the changes in the banks before the gyrus and fundus in the progression to AD.

The IPL has demonstrated laterality, both in correlations between volume and cognitive status (Keilp et al., 1996) and in atrophy related to progression to AD (Whitwell et al., 2008), with a predilection for the left IPL. This study was consistent with these findings, as the only significant difference between normal controls and MCI participants was in the average cortical thickness of the banks of the left IPL. However, significant differences between MCI and AD subjects occurred only in the right hemisphere in all measures of the subregions of the IPL (except for the GMV of the fundus), suggesting the right IPL may become more affected as subjects progress from MCI to AD. While the GMV of the fundus did not demonstrate significant differences between groups, it was found to be a predictor of future conversion from MCI to AD when combined with BNT, AV Delay, and Digit Span Backwards.

The second objective in this study was to investigate relationships between these subregions and neuropsychological performance. When considering NP performance, the only NP scores that were significantly different between the NC and MCI groups were auditory verbal learning immediate and delayed, Categories, Digit Symbol, and the Boston Naming Test. Significant correlations with the ACT of the banks of the left IPL (the only IPL subregion to demonstrate significant differences between NC and MCI) were found only with Auditory Verbal Learning Delay. There were no normal subjects included in this study who converted to MCI, and so it was not possible to determine predictors for conversion from normal to MCI. However, these data suggest that the above-mentioned test of memory may be sensitive to detecting the progression from normal to MCI.

When assessing MCI stable versus converters, the best predictors of future conversion were the Boston Naming Test, Digit Span Backwards, and GMV of the fundus of the right IPL. When the measure of the IPL were combined with those of the entorhinal cortex and hippocampus and entered into the discriminant function analysis, the IPL fell out of the results, leaving the TSA of the left entorhinal cortex to be the best predictor of conversion. However, the results of this second discriminant function analysis provided a less accurate prediction of future stable versus converters (here stable subjects were predicted with 84.6% accuracy compared with 92.3%, and converters were predicted with 80% compared with 100% accuracy). This suggests that measures of the IPL are independent of entorhinal and hippocampal measures when comparing between groups and future conversion to AD.

To our knowledge no studies have investigated the differential effects of these subregions of the IPL in the progression to AD. This research suggests that detecting subtle changes within these subregions may identify individuals in the earliest stages of AD. These measures, combined with neuropsychological data, may provide useful biomarkers for future development of AD.

Limitations of this study included a small study population, due time intense tracing of each subregion of the IPL. It is possible that these initial tracings may be used to create an automated label for these subregions that can be incorporated into FreeSurfer for this specific dataset and could be used to assess the entire ADNI study population in the future.

In addition, only the baseline visits of these participants were evaluated. While progression from MCI to AD was evaluated, the longitudinal change occurring in these subregions was not evaluated. Further investigation into the changes that may occur within each subregion of the IPL as participants are followed throughout the 36-month period of the ADNI project would likely provide further insight into the role of the IPL in the progression to AD.

Disclosure statement

There are no actual or potential conflicts of interest for authors regarding this study.

Acknowledgements

Data collection and sharing for this project was funded by the ADNI (National Institutes of Health, Grant U01 AG024904). ADNI is funded by the National Institute on Aging, the National Institute of Biomedical Imaging and Bioengineering, and through generous contributions from the following: Abbott, AstraZeneca AB, Bayer Schering Pharma AG, Bristol-Myers Squibb, Eisai Global Clinical Development, Elan Corporation, Genentech, GE Healthcare, GlaxoSmithKline, Innogenetics, Johnson and Johnson, Eli Lilly, and Co., Medpace, Inc., Merck and Co., Inc., Novartis AG, Pfizer, Inc, F. Hoffman-La Roche, Schering-Plough, Synarc, Inc., and Wyeth, as well as nonprofit partners the Alzheimer's Association and Alzheimer's Drug

Discovery Foundation, with participation from the US Food and Drug Administration. Private sector contributions to ADNI are facilitated by the Foundation for the National Institutes of Health (www.fnih.org, www.fnih.org/, www.fnih.org, www.fnih.org/). The grantee organization is the Northern California Institute for Research and Education, and the study is coordinated by the Alzheimer's Disease Cooperative Study at the University of California, San Diego. ADNI data are disseminated by the Laboratory for Neuro Imaging at the University of California, Los Angeles. This research was also supported by NIH Grants P30 AG010129, K01 AG030514, and the Dana Foundation. Funding for this specific project was supported by NIH grant AG000277.

References

Bennett, D.A., Schneider, J.A., Bienias, J.L., Evans, D.A., Wilson, R.S., 2005. Mild cognitive impairment is related to alzheimer disease pathology and cerebral infarctions. Neurology 64, 834–841.

Braak, H., Braak, E., 1991. Neuropathological staging of alzheimer-related changes. Acta Neuropathol 82, 239–259.

Chochon, F., Cohen, L., van de Moortele, P.F., Dehaene, S., 1999. Differential contributions of the left and right inferior parietal lobules to number processing. J Cognit Neurosci 11, 617–630.

Clower, D.M., West, R.A., Lynch, J.C., Strick, P.L., 2001. The inferior parietal lobule is the target of output from the superior colliculus, hippocampus, and cerebellum. J Neurosci 21, 6283–6291.

Dale, A.M., Fischl, B., Sereno, M.I., 1999. Cortical surface-based analysis. I. segmentation and surface reconstruction. Neuroimage 9, 179–194.

Dale, A.M., Sereno, M.I., 1993. Improved localization of cortical activity by combining EEG and MEG with MRI cortical surface reconstruction: A linear approach. J Cognit Neurosci 5, 162–176.

Desikan, R.S., Cabral, H.J., Fischl, B., Guttmann, C.R., Blacker, D., Hyman, B.T., Albert, M.S., Killiany, R.J., 2009. Temporoparietal MR imaging measures of atrophy in subjects with mild cognitive impairment that predict subsequent diagnosis of alzheimer disease. AJNR Am J Neuroradiol 30, 532–538.

Desikan, R.S., Fischl, B., Cabral, H.J., Kemper, T.L., Guttmann, C.R., Blacker, D., Hyman, B.T., Albert, M.S., Killiany, R.J., 2008. MRI measures of temporoparietal regions show differential rates of atrophy during prodromal. Adv Neurol 71, 819–825.

Desikan, R.S., Segonne, F., Fischl, B., Quinn, B.T., Dickerson, B.C., Blacker, D., Buckner, R.L., Dale, A.M., Maguire, R.P., Hyman, B.T., Albert, M.S., Killiany, R.J., 2006. An automated labeling system for subdividing the human cerebral cortex on MRI scans into gyral based regions of interest. Neuroimage 31, 968–980.

Devanand, D.P., Habeck, C.G., Tabert, M.H., Scarmeas, N., Pelton, G.H., Moeller, J.R., Mensh, B.D., Tarabula, T., Van Heertum, R.L., Stern, Y., 2006. PET network abnormalities and cognitive decline in patients with mild cognitive impairment. Neuropsychopharmacology 31, 1327–1334.

Ding, S.L., Van Hoesen, G., Rockland, K.S., 2000. Inferior parietal lobule projections to the presubiculum and neighboring ventromedial temporal cortical areas. J Comp Neurol 425, 510–530.

Fan, Y., Resnick, S.M., Wu, X., Davatzikos, C., 2008. Structural and functional biomarkers of prodromal alzheimer's disease: A high-dimensional pattern classification study. Neuroimage 41, 277–285.

Fischl, B., Dale, A.M., 2000. Measuring the thickness of the human cerebral cortex from magnetic resonance images. Proc Natl Acad Sci USA 97, 11050–11055.

Fischl, B., Liu, A., Dale, A.M., 2001. Automated manifold surgery: Constructing geometrically accurate and topologically correct models of the human cerebral cortex. IEEE Trans Med Imaging 20, 70–80.

Fischl, B., Salat, D.H., Busa, E., Albert, M., Dieterich, M., Haselgrove, C., van der Kouwe, A., Killiany, R., Kennedy, D., Klaveness, S., Montillo, A., Makris, N., Rosen, B., Dale, A.M., 2002. Whole brain segmentation: Automated labeling of neuroanatomical structures in the human brain. Neuron 33, 341–355.

Fischl, B., Salat, D.H., van der Kouwe, A.J., Makris, N., Segonne, F., Quinn, B.T., Dale, A.M., 2004a. Sequence-independent segmentation of magnetic resonance images. Neuroimage 23 suppl 1, S69–S84.

Fischl, B., Sereno, M.I., Dale, A.M., 1999a. Cortical surface-based analysis. II: Inflation, flattening, and a surface-based coordinate system. Neuroimage 9, 195–207.

Fischl, B., Sereno, M.I., Tootell, R.B., Dale, A.M., 1999b. High-resolution intersubject averaging and a coordinate system for the cortical surface. Hum Brain Mapp 8, 272–284.

Fischl, B., van der Kouwe, A., Destrieux, C., Halgren, E., Segonne, F., Salat, D.H., Busa, E., Seidman, L.J., Goldstein, J., Kennedy, D., Caviness, V., Makris, N., Rosen, B., Dale, A.M., 2004b. Automatically parcellating the human cerebral cortex. Cereb Cortex 1991, 11–22.

Fox, N.C., Crum, W.R., Scahill, R.I., Stevens, J.M., Janssen, J.C., Rossor, M.N., 2001. Imaging of onset and progression of alzheimer's disease with voxel-compression mapping of serial magnetic resonance images. Lancet 358, 201–205.

Grossman, M., Payer, F., Onishi, K., White-Devine, T., Morrison, D., D'Esposito, M., Robinson, K., Alavi, A., 1997. Constraints on the cerebral basis for semantic processing from neuroimaging studies of alzheimer's disease. J Neurol Neurosurg Psychiatry 63, 152–158.

Han, X., Jovicich, J., Salat, D., van der Kouwe, A., Quinn, B., Czanner, S., Busa, E., Pacheco, J., Albert, M., Killiany, R., Maguire, P., Rosas, D., Makris, N., Dale, A., Dickerson, B., Fischl, B., 2006. Reliability of MRI-derived measurements of human cerebral cortical thickness: The effects of field strength, scanner upgrade and manufacturer. Neuroimage 32, 180–194.

Jack, C.R., Jr, Bernstein, M.A., Fox, N.C., Thompson, P., Alexander, G., Harvey, D., Borowski, B., Britson, P.J., Whitwell, L., J., Ward, C., Dale, A.M., Felmlee, J.P., Gunter, J.L., Hill, D.L., Killiany, R., Schuff, N., Fox-Bosetti, S., Lin, C., Studholme, C., deCarli, C.S., Krueger, G., Ward, H.A., Metzger, G.J., Scott, K.T., Mallozzi, R., Blezek, D., Levy, J., Debbins, J.P., Fleisher, A.S., Albert, M., Green, R., Bartzokis, G., Glover, G., Mugler, J., Weiner, M.W., 2008. The alzheimer's disease neuroimaging initiative (ADNI): MRI methods. J Magn Reson Imaging JMRI 27, 685–691.

Jovicich, J., Czanner, S., Greve, D., Haley, E., van der Kouwe, A., Gollub, R., Kennedy, D., Schmitt, F., Brown, G., Macfall, J., Fischl, B., Dale, A., 2006. Reliability in multi-site structural MRI studies: Effects of gradient non-linearity correction on phantom and human data. Neuroimage 30, 436–443.

Kaplan, E.F., Goodglass, H., Weintraub, S., 1983. The Boston Naming Test. Lea & Febiger, Philadelphia.

Keilp, J.G., Alexander, G.E., Stern, Y., Prohovnik, I., 1996. Inferior parietal perfusion, lateralization, and neuropsychological dysfunction in alzheimer's disease. Brain Cogn 32, 365–383.

Markesbery, W.R., Schmitt, F.A., Kryscio, R.J., Davis, D.G., Smith, C.D., Wekstein, D.R., 2006. Neuropathologic substrate of mild cognitive impairment. Arch Neurol 63, 38–46.

McKhann, G., Drachman, D., Folstein, M., Katzman, R., Price, D., Stadlan, E.M., 1984. Clinical diagnosis of alzheimer's disease: Report of the NINCDS-ADRDA work group under the auspices of department of health and human services task force on alzheimer's disease. Neurology 34, 939–944.

Morris, J.C., 1993. The clinical dementia rating (CDR): Current version and scoring rules. Neurology 43, 2412–2414.

Morris, J.C., Storandt, M., Miller, J.P., McKeel, D.W., Price, J.L., Rubin, E.H., Berg, L., 2001. Mild cognitive impairment represents early-stage alzheimer disease. Arch Neurol 58, 397–405.

Nelson, P.T., Abner, E.L., Scheff, S.W., Schmitt, F.A., Kryscio, R.J., Jicha, G.A., Smith, C.D., Patel, E., Markesbery, W.R., 2009. Alzheimer's-type neuropathology in the precuneus is not increased relative to other areas of neocortex across a range of cognitive impairment. Neurosci Lett 450, 336–339.

Petersen, R.C., Parisi, J.E., Dickson, D.W., Johnson, K.A., Knopman, D.S., Boeve, B.F., Jicha, G.A., Ivnik, R.J., Smith, G.E., Tangalos, E.G., Braak, H., Kokmen, E., 2006. Neuropathologic features of amnestic mild cognitive impairment. Arch Neurol 63, 665–672.

Reitan, R.M., 1958. Validity of the trail making tests as an indicator of organic brain damage. Percept Mot Skills 8, 253–266.

Remy, F., Mirrashed, F., Campbell, B., Richter, W., 2005. Verbal episodic memory impairment in alzheimer's disease: A combined structural and functional MRI study. Neuroimage 25, 253–266.

Rey, A., 1964. L'examen clinique en psychologie. Presses Universitaires de France. Paris, France.

Rosen, W.G., Mohs, R.C., Davis, K.L., 1984. A new rating scale for alzheimer's disease. Am J Psychiatry 141, 1356–1364.

Scahill, R.I., Schott, J.M., Stevens, J.M., Rossor, M.N., Fox, N.C., 2002. Mapping the evolution of regional atrophy in alzheimer's disease: Unbiased analysis of fluid-registered serial MRI. Proc Natl Acad Sci USA 99, 4703–4707.

Scarmeas, N., Habeck, C.G., Zarahn, E., Anderson, K.E., Park, A., Hilton, J., Pelton, G.H., Tabert, M.H., Honig, L.S., Moeller, J.R., Devanand, D.P., Stern, Y., 2004. Covariance PET patterns in early alzheimer's disease and subjects with cognitive impairment but no dementia: Utility in group discrimination and correlations with functional performance. Neuroimage 23, 35–45.

Schroeter, M.L., Stein, T., Maslowski, N., Neumann, J., 2009. Neural correlates of alzheimer's disease and mild cognitive impairment: A systematic and quantitative meta-analysis involving 1351 patients. Neuroimage 47, 1196–1206.

Segonne, F., Dale, A.M., Busa, E., Glessner, M., Salat, D., Hahn, H.K., Fischl, B., 2004. A. hybrid approach to the skull stripping problem in MRI. Neuroimage 22, 1060–1075.

Segonne, F., Pacheco, J., Fischl, B., 2007. Geometrically accurate topology-correction of cortical surfaces using nonseparating loops. IEEE Trans Med Imaging 26, 518–529.

Sled, J.G., Zijdenbos, A.P., Evans, A.C., 1998. A nonparametric method for automatic correction of intensity nonuniformity in MRI data. IEEE Trans Med Imaging 17, 87–97.

Small, G.W., Ercoli, L.M., Silverman, D.H., Huang, S.C., Komo, S., Bookheimer, S.Y., Lavretsky, H., Miller, K., Siddarth, P., Rasgon, N.L., Mazziotta, J.C., Saxena, S., Wu, H.M., Mega, M.S., Cummings, J.L., Saunders, A.M., Pericak-Vance, M.A., Roses, A.D., Barrio, J.R., Phelps, M.E., 2000. Cerebral metabolic and cognitive decline in persons at genetic risk for alzheimer's disease. Proc Natl Acad Sci USA 97, 6037–6042.

Tranfaglia, C., Palumbo, B., Siepi, D., Sinzinger, H., Parnetti, L., 2009. Semi-quantitative analysis of perfusion of brodmann areas in the differential diagnosis of cognitive impairment in alzheimer's disease, fronto-temporal dementia and mild cognitive impairment. Hellenic J Nucl Med 12, 110–114.

Van Hoesen, G., Pandya, D.N., 1975. Some connections of the entorhinal (area 28) and perirhinal (area 35) cortices of the rhesus monkey. I. temporal lobe afferents. Brain Res 95, 1–24.

Wechsler, D, 1987. Wechsler memory scale-revised. Psychological Corporation, San Antonio, Texas.

Whitwell, J.L., Petersen, R.C., Negash, S., Weigand, S.D., Kantarci, K., Ivnik, R.J., Knopman, D.S., Boeve, B.F., Smith, G.E., Jack, C.R., Jr, 2007. Patterns of atrophy differ among specific subtypes of mild cognitive impairment. Arch Neurol 64, 1130–1138.

Whitwell, J.L., Shiung, M.M., Przybelski, S.A., Weigand, S.D., Knopman, D.S., Boeve, B.F., Petersen, R.C., Jack, C.R., Jr, 2008. MRI patterns of atrophy associated with progression to AD in amnestic mild cognitive impairment. Neurology 70, 512–520.